LATTICE BOLTZMANN SIMULATION OF DYNAMIC OXYGEN ADSORPTION IN COAL BASED ON FRACTAL CHARACTERISTICS

by

Zijin LI[a], Huiyan GUO[a], Hongxiang ZHOU[a], Chang GUO[b], Rongshan NIE[2], and Xiaoyu LIANG[a,b*]

[a] College of Metrology and Measurement Engineering, China Jiliang University, Hangzhou, China
[b] College of Quality and Safety Engineering, China Jiliang University, Hangzhou, China

Original scientific paper
https://doi.org/10.2298/TSCI220718202L

The issue of coal spontaneous combustion greatly threatens the production safety of coal mining, storage, and transportation. It is significant to study oxygen adsorption understand the mechanism of coal spontaneous combustion. In this paper, based on the fractal dimension of coal and the self-similar fractal geometry, the internal pore structure of coal is modeled. Then, the lattice Boltzmann method is employed to conduct the numerical simulation of oxygen adsorption in coal. Compared with the existing experimental data and numerical simulation, the lattice Boltzmann method is verified to be correct. The numerical results indicate that in the process of oxygen adsorption in coal, the preferential flow occurs when the large pores connect to the channel. In the meantime, the large diffusion coefficient leads to an early time for adsorption equilibrium. The oxygen adsorption increases with an increased adsorption rate constant. Pore structure plays a significant role in the adsorption behavior of oxygen in coal. The results can provide theoretical support for reducing coal spontaneous combustion and ensuring coal mine safety in production.

Key words*: coal oxygen adsorption, fractal dimension, pore structure, lattice Boltzmann method*

Introduction

The study of coal spontaneous combustion began in the 17th century and has been extensively studied over the years, with studies resulting in pyrite induction theory, bacteria induction theory, phenol-based induction theory, coal-oxygen composite theory, and so on being the most prominent. Among them, the coal-oxygen composite theory is generally accepted by most academics [1]. According to this theory, the main reason for coal spontaneous combustion is the complex pore structure of coal as a complex porous medium, which has a relatively strong adsorption ability for oxygen [2]. Therefore, the process of oxidative spontaneous combustion reaction that occurs during the contact between coal and oxygen is mainly the repetition of physical adsorption, chemical adsorption, and chemical reaction, in which the stage of physical adsorption of oxygen in coal is the beginning of the reaction between coal and oxygen [3].

To study the oxygen adsorption characteristics of coal, the pore structure distribution in coal must be obtained first. At present, experimental methods and numerical construction methods are generally used. The experimental method is to obtain real geometric images di-

* Corresponding author, e-mail: xyliang@cjlu.edu.cn

rectly by scanning technology. The experimental method mainly included X-ray computed tomography [4], magnetic resonance imaging [5], SEM [6], and synchrotron microtomography [7]. The numerical construction method simulates the formation process of pore and fracture micro-structure using mathematical and physical equations and existing computer technology. Some popular methods include Monte-Carlo processes [8], discrete element method [9], and quartet structure generation set method [10]. Traditional construction models are commonly based on simple physical and geometric assumptions and therefore, are incapable of revealing the complex characteristics of pores and cracks. However, porous media shows statistical self-similar fractal characteristics, and the fractal theory can effectively describe the distribution characteristics of complex pore structures in porous media [11]. The pore structure of coal micropores accords with fractal theory. As a result, Lv *et al*. [12] combined self-similar fractal geometry with the fractal dimension of coal to explore the phenomenon of gas adsorption in coal.

At the same time, much effort has been devoted to using CFD methods to evaluate the gas-solid adsorption process inside the porous media [13]. Compared with the traditional hydrodynamics methods, the lattice Boltzmann method (LBM), which has developed rapidly in recent years, has unique advantages in dealing with complex boundaries in porous media, so it has been widely used in the simulation of the transmission process in porous media [14]. Zhou *et al.* [15] proved that LBM can be used in the gas-solid adsorption process in randomly constructed porous media. Wang *et al.* [16] used LBM to simulate the adsorption of mixed gases, and Lei *et al.* [17] constructed porous media with inhomogeneous porosity for adsorption simulation. More importantly, as LBM and other simulation methods applying to complex boundaries are used, a large number of fluid and pore structure wall nodes in the porous medium can be processed more effectively [18]. Many scholars have considered utilizing fractal theory to construct porous media and combining LBM to carry out the numerical simulation. The flow characteristics in the fractal structure are consistent with the theoretical results [19].

Despite various efforts that have been made to reveal the behavior of gas in porous media, it is still essential to construct porous structures based on fractal dimension study the flow and adsorption of gas on pore-scale. In addition, more research is needed on the dynamic adsorption performance. Especially, it is currently unknown how the characteristics of pore structure affect the adsorption behavior. Therefore, the pore structure of coal is modeled based on fractal dimension and self-similar Sierpinski carpet model. The LBM is used to simulate the process of oxygen adsorption in coal on the pore-scale, and the dynamic adsorption performance of oxygen adsorption in coal is comprehensively analyzed. The results can provide a reference for the mechanism research of coal spontaneous combustion and coal mine fire prevention.

The self-similar Sierpinski carpet model

As a porous medium, coal has a complicated pore structure. The traditional Euclidean geometry theory has limitations in describing pore structure. Researchers discovered that coal has self-similar characteristics, and its pore structure can be quantitatively characterized by the fractal model. The self-similar Sierpinski carpet model was adopted to simulate the microstructure of coal porous media [12]. Figure 1 shows two types of Sierpinski carpet models, first-order, fig. 1(a), and second-order, fig. 1(b). The first-order carpet model can be constructed by cutting the center of the square. The second-order carpet model can be obtained by translating and expanding the first-order carpet model. Black and white represent coal solids and pores in coal media, respectively.

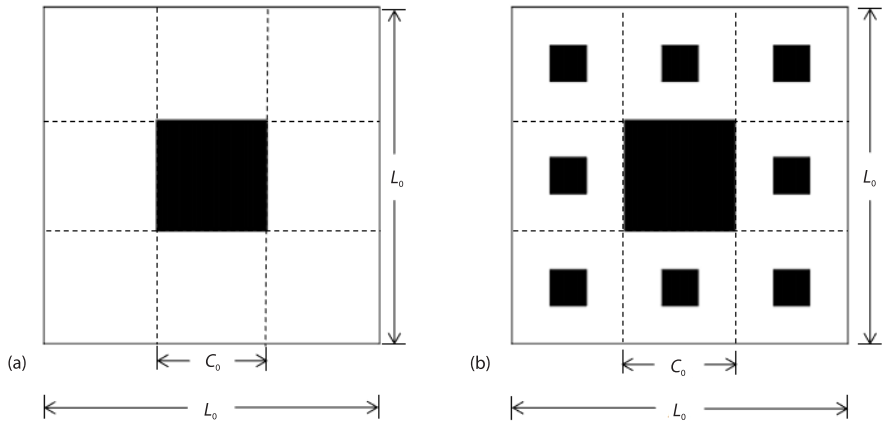

Figure 1. Sierpinski carpet model and regional division;
(a) first-order Sierpinski carpet model and (b) second-order Sierpinski carpet model

This equation can be used to calculate the Sierpinski carpet model's fractal dimension, D_f, and porosity, ε:

$$D_f = \frac{\ln\left(L_0^2 - C_0^2\right)}{\ln\left(L_0\right)} \tag{1}$$

$$\varepsilon = \left(\frac{L_0^2 - C_0^2}{L_0^2}\right)^n \tag{2}$$

The order of the Sierpinski carpet model is indicated by the positive number n, C_0 is the cutting size, and L_0 is the side length. The experimental results [12] indicate that coal has a fractal dimension in two dimensions that ranges from 1.0-2.0. Equation (1) shows that by varying the cutting size C_0 or side length L_0, the self-similar Sierpinski carpet model with varied fractal dimensions will be created. By referring to the different cutting sizes C_0 and side lengths L_0 of the self-similar Sierpinski carpet constructed by the aforementioned work, the self-similar Sierpinski carpet model with different fractal dimensions is modeled as shown in tab. 1. Figure 2 shows the first-order Sierpinski carpet model with C_0/L_0 of 3/13, 5/13, 7/13, and 9/13.

Simulation method and model verification

Mathematical equation for adsorption process

The mass transfer of simulated coal adsorbed oxygen includes adsorbent pore, adsorbent surface, and adsorbent interior. The governing equation between adsorbent pores:

$$\frac{\partial C}{\partial t} + u\frac{\partial C}{\partial x} + v\frac{\partial C}{\partial y} = D_\mathrm{s}\left(\frac{\partial^2 C}{\partial x^2} + \frac{\partial^2 C}{\partial y^2}\right) \tag{3}$$

where C is the gas phase concentration on the adsorbent surface and D_s – the diffusion coefficient of adsorbate in adsorbent pores. The adsorption behavior usually occurs on the surface of the adsorbent when the adsorbate contacts the adsorbent. The Langmuir adsorption kinetics was employed to explain the surface mass transfer of adsorbents, which is shown:

$$D_\mathrm{s} = \frac{\partial C}{\partial \boldsymbol{n}} = \frac{\partial N}{\partial t} = k_1 C\left(N_m - N\right) - k_{-1}N \tag{4}$$

where $\boldsymbol{n}$ is the normal direction of the boundary, k_1 and k_{-1} are the adsorption and desorption rate constants of oxygen, N_m – the saturated adsorption amount when the adsorption reaches equilibrium, and N – the adsorption amount.

When the adsorbate is captured by the adsorbent surface, it continues to diffuse inside the adsorbent. For the adsorbent with internal diffusion, the homogeneous solid diffusion model is adopted to deal with mass transfer:

$$\frac{\partial N}{\partial t} = D_{\mathrm{sp}}\left(\frac{\partial^2 N}{\partial x^2} + \frac{\partial^2 N}{\partial y^2}\right) \tag{5}$$

where D_{sp} is the diffusion coefficient within the adsorbent.

Table 1. The parameters of the self-similar Sierpinski carpet models (L_0 = 26 nm)

Model name	C_0/L_0	D_f	ε	n
S1	3/13	1.979	0.946	1
S2	3/13	1.979	0.896	2
S3	5/13	1.938	0.852	1
S4	5/13	1.938	0.726	2
S5	7/13	1.866	0.710	1
S6	7/13	1.866	0.504	2
S7	9/13	1.746	0.521	1
S8	9/13	1.746	0.271	2
S9	1/3	1.893	0.889	1
S10	1/3	1.893	0.790	2
S11	1/3	1.893	0.702	3
S12	1/5	1.975	0.960	1
S13	1/5	1.975	0.922	2
S14	1/5	1.975	0.855	3
S15	3/5	1.723	0.640	1
S16	1/7	1.989	0.980	1
S17	3/7	1.896	0.816	1
S19	1/9	1.994	0.988	1
S20	5/9	1.832	0.691	1

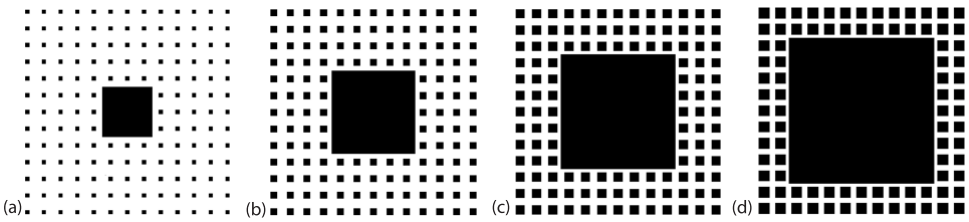

Figure 2. The second-order of self-similar Sierpinski carpet models with C_0/L_0 of 3/13 (a), 5/13 (b), 7/13 (c), and 9/13 (d)

The lattice Boltzmann method

Zhou *et al.* [15] simulated fluid-flow and adsorption behavior at the pore-scale by improving and optimizing the LBM method. Along this line, the multiple relaxation time mod-

el with the D2Q9 scheme is applied to simulate the flow. The evolution equation that includes collision and flow steps:

$$\boldsymbol{f}\left(\boldsymbol{r}_i+\Delta t\boldsymbol{e}_i,t+\Delta t\right)-\boldsymbol{f}\left(\boldsymbol{r}_i,t\right)=-[\mathrm{M}]^{-1}[\hat{\mathrm{S}}]\left[\boldsymbol{m}\left(\boldsymbol{r},t\right)-\boldsymbol{m}^{\mathrm{eq}}\left(\boldsymbol{r},t\right)\right] \tag{6}$$

where $\boldsymbol{r}_i$ is the particle position, Δt – the time step, and $\boldsymbol{e}_i$ is the discrete velocity direction, f – the column vector, including nine velocity distribution functions, [M] is a 9×9 matrix, and the velocity distribution function f is transformed into the velocity moments $\boldsymbol{m}$ by the linear mapping:

$$\boldsymbol{m}=[\mathrm{M}]\times\boldsymbol{f}\quad\text{or}\quad\boldsymbol{f}=[\mathrm{M}]^{-1}\times\boldsymbol{m} \tag{7}$$

Pierre and Luo [20] contains the format of matrix [M] and equilibrium moments $\boldsymbol{m}^{\mathrm{eq}}$. The $[\hat{\mathrm{S}}]$ is the nine-order diagonal collision matrix of relaxation rate, expressed in compact representation:

$$[\hat{\mathrm{S}}]=diag\left(1.0,1.1,1.1,1.0,8\frac{2-s_\nu}{8-s_\nu},s_\nu,s_\nu\right) \tag{8}$$

where ν is kinetic viscosity and $s_\nu = 2/(1 + 6\nu)$.

The convection effect only occurs between the pores of adsorbate and is disregarded within adsorbate. The adsorption reaction process takes place when the adsorbate comes into contact with the adsorbent, rather than between the pores of the adsorbent. As a result, it is assumed that the transportation of adsorbate between pores does not affect local velocity. The mass transfer in the adsorbent is completed by-passive scalar concentration. Hence, using the passive scalar characteristic, the mass transfer adopts the single relaxation time model with the D2Q5 scheme, which is described:

$$g_i\left(\boldsymbol{r}_i+\Delta t\boldsymbol{e}_i,t+\Delta t\right)-g_i\left(\boldsymbol{r},t\right)=-\frac{1}{\tau_{\mathrm{s}}}\left[g_i\left(\boldsymbol{r},t\right)-g_i^{\mathrm{eq}}\left(\boldsymbol{r},t\right)\right] \tag{9}$$

where g_i is the concentration distribution function and τ_{s} is the relaxation time. The equilibrium distribution function g_i^{eq} is denoted:

$$g_i^{\mathrm{eq}}\left(\boldsymbol{r},t\right)=C_{\mathrm{s}}\omega_i\left(1+\frac{\boldsymbol{e}_i u}{c_{\mathrm{s}}^2}\right) \tag{10}$$

where ω_i is the weight coefficient and c_{s} is the sound speed. For the D2Q5 model, $\omega_0 = 1/3$, $\omega_{1\text{-}4} = 1/6$. The mass diffusion coefficient D_{s} and the gas concentration C_{s} are obtained:

$$D_{\mathrm{s}}=c_{\mathrm{s}}^2\left(\tau_{\mathrm{s}}-0.5\right)\Delta t \tag{11}$$

$$C_{\mathrm{s}}=\sum_i g_i \tag{12}$$

For the numerical simulation of coal oxygen adsorption, the treatment of its boundary conditions plays a crucial role. Guo *et al.* [21] proposed the non-equilibrium extrapolation method, which is suitable for the hydrodynamic boundary conditions of channel domain boundaries and fluid-solid surfaces. The concentration distribution function is obtained:

$$g_{i(e_i n>0)}=\frac{\left[C_\omega-\sum_{i(\boldsymbol{e}_i n\le 0)} g_i\right]\omega_i}{\sum_{i(\boldsymbol{e}_i n\le 0)}\omega_i} \tag{13}$$

The critical issue is determining the boundary concentration, C_ω. The entrance C_ω is known. For the condition of concentration flux, the exact three-point finite-difference scheme is presented, and the concentration gradient is introduced:

$$\frac{\partial C_\omega}{\partial \boldsymbol{n}} = \frac{3C_\omega - 4C_{(j,n+1)} + C_{(j,n+2)}}{2\Delta n} \tag{14}$$

The upper wall and the bottom wall of the outlet, $\partial C/\partial \boldsymbol{n}$ are zero under the condition of no concentration flux. At the contact surface between adsorbent and adsorbate, the Langmuir kinetic adsorption reaction in eq. (5) is combined with eq. (15) to solve C_ω.

The overall adsorptive capacity indicators of the dynamic adsorption process can be explained by calculating the average adsorption amount of all the calculated points on the adsorbent in the transient state. The average value of the adsorption amount $N_{(t)}$ is calculated:

$$\bar{N}_{(t)} = \frac{\sum_i \sum_j N_{(t)(i,j)}}{\sum_i \sum_j N_m} \tag{15}$$

where $N_{(t)(i,j)}$ denotes the amount of adsorption at the calculated point (i, j) at time t.

Verification of grid resolution

Considering that the grid size has a direct impact on the error of numerical simulation, it is necessary to carry out a sensitivity analysis on the grid size. Four alternative grids types are selected: $N_x \times N_y = 178 \times 178$, 338×338, 498×498, and 658×658, which correspond to the figs. 3(a)-3(d) in the current research, to ensure that the numerical results obtained are independent of the grid size. See fig. 3 for the velocity contours in four cases. Obviously, once the number of grids increases to 498×498, as in fig. 3(c), there is essentially little difference between the velocity contour and fig. 3(d). Figure 4 shows the comparison of the velocity distribution along the y-axis of the center line of the calculation area. With the expansion of grid size, the velocity distribution near the middle declined steadily into a curve. In addition, the maximum flow rates under the four cases are 0.008373 m/s, 0.010877 m/s, 0.012550 m/s, and 0.012704 m/s, respectively. The relative difference among cases gradually decreased from 23.02-1.21%. Therefore, the analysis proves that the grid size of $N_x \times Ny = 498 \times 498$ is the most practical to ensure numerical accuracy.

Verification of the lattice Boltzmann model

To verify the LBM model, the self-similar Sierpinski carpet model S10 in tab. 1 is adopted to the numerical simulation. According to the analysis of grid resolution, the grid size is $N_x \times N_y = 498 \times 498$. The inlet speed is 0.589 m/s, and the inlet gas concentration is 44.66 mol/m^3. Coal has a density of 1400 kg/m^3, while oxygen has a density of 1.429 kg/m^3. On the upper and bottom walls of the outlets, a zero-concentration flux condition is applied. The results of LBM simulation are compared with the experimental data of oxygen adsorption in coal [21] and the result is shown in fig. 5. The simulation findings follow the same trend as the experimental data, demonstrating the suitability of the model in this work for the measured data. As a result, there was enough trust in the comparison and verification apply the LBM to simulate the adsorption of gas in porous media. The simulated adsorption amount is marginally larger than the metrical results, which may be due to the fact that the unconnected pores are not taken into account in the current numerical simulation.

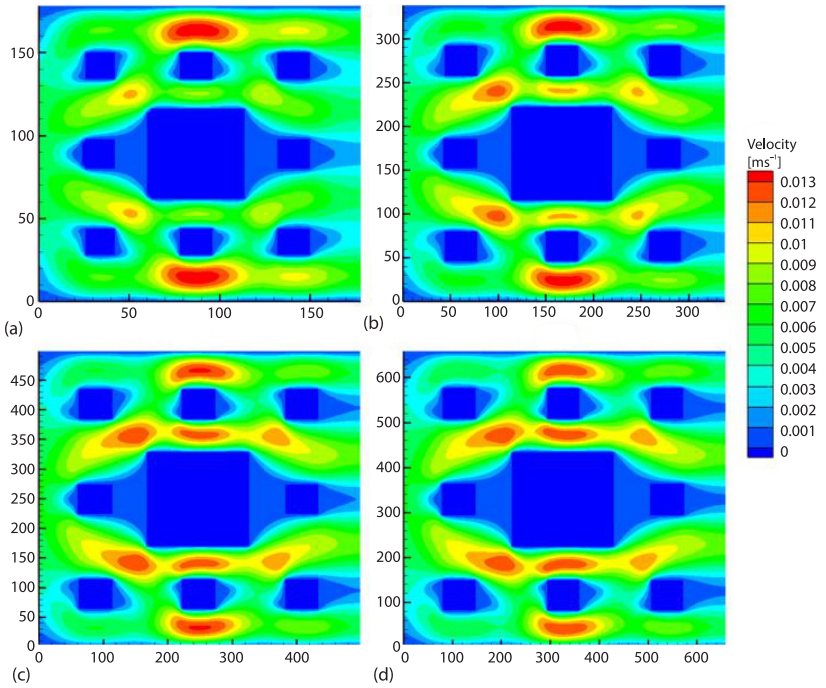

Figure 3. Velocity contour at four different grids types case; (a) $N_x \times N_y = 178 \times 178$, (b) $N_x \times N_y = 338 \times 338$, (c) $N_x \times N_y = 498 \times 498$, and (d) $N_x \times N_y = 658 \times 658$

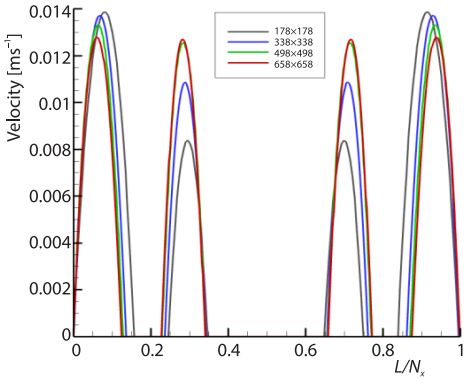

Figure 4. Comparison of velocity distribution at the centerline of the computational domain along the *y*-axis for the four cases with different grid numbers

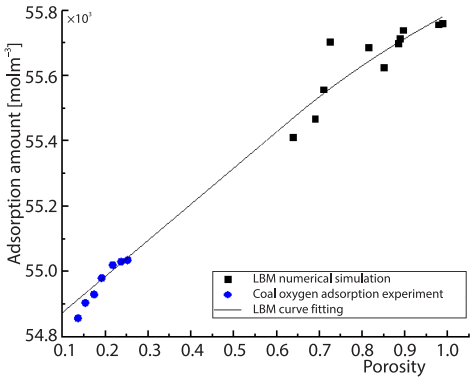

Figure 5. Comparison between numerical simulation results and experimental data

Results and discussion

Dominant channel

The coal pore structure S4 in tab. 1 is applied to the numerical simulation of oxygen adsorption. Figure 6 shows the distribution of transient oxygen flow rate at 0.0255 μs. It can be seen that there are dominant channels for oxygen in coal during oxygen adsorption

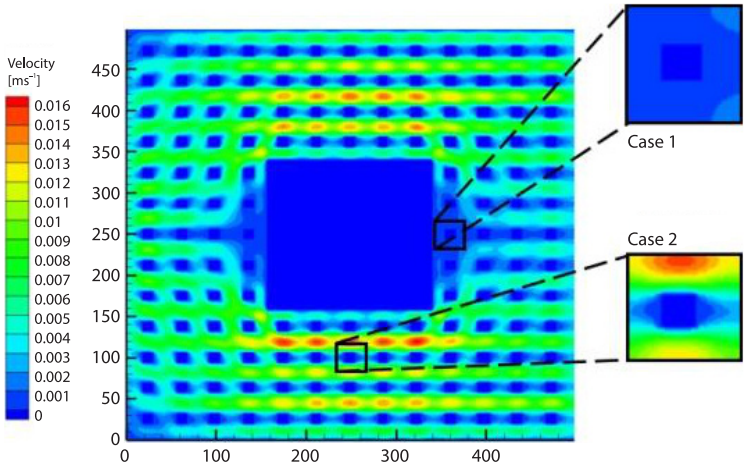

Figure 6. Distribution of transient oxygen flow rate at 0.0255 μs

process, and oxygen flows preferentially along the channels formed by the pores with good connectivity. However, not all large pores in coal can be the dominant channel. Oxygen flow rate and adsorption amount are small around the closed or poorly connected pores. In the process of oxygen adsorption in coal, the dominant channel is formed in the connections of large pores, and the oxygen flow rate in the dominant channel is much higher than in the other parts. In the equilibrium of adsorption, the adsorption amount in the wall of the dominant channel (Case 1) is 0.72 g/cm^3, which is larger than the adsorption amount in the wall of the unconnected pores beyond the dominant channel (Case 2), which is 0.50 g/cm^3.

Diffusion coefficient

In order to explore the influence of diffusion coefficient on coal oxygen adsorption, the coal pore structures S3, S5, S12, S16, and S20 in tab. 1 are selected. Figure 7 takes the S5 as an example, showing the relationship between different diffusion coefficients, D_s, and average adsorption amount. It can be seen that the maximum adsorption velocity of oxygen in coal appears when the diffusion coefficient is 0.833. It takes the least time for adsorption reach equilibrium at this point, which is 0.062 μs. The larger the diffusion coefficient, the less time it takes for adsorption reach equilibrium. However, the average value of oxygen saturation adsorption of coal is almost constant with the changing of diffusion coefficient. Figure 8 shows the relationship between diffusion coefficient and adsorption rate at 0.055 μs under different porosity. With the progress of the adsorption, the adsorption rate of oxygen adsorbed by coal with different diffusion coefficients is different at the same time. The larger the diffusion coefficient, the bigger the adsorption velocity and the higher the adsorption rate. The adsorption rate rises as porosity increases. These phenomena are since during the process of coal oxygen adsorption, the mass transfer within pores mainly depends on the convection and diffusion in the fluid domain, and the mass transfer within particles mainly depends on the diffusion coefficient of gas within the coal, among which the diffusion within particles plays a leading role in the mass transfer process. The larger the diffusion coefficient, the faster the adsorption reaches equilibrium.

Adsorption rate constant

The adsorption rate constant indicates significant effect on the oxygen adsorption in coal. The coal pore structures are S3, S5, S12, S16, and S20 in tab. 1. Figure 9 takes the S5 as

an example, showing the relationship between adsorption rate constant and average adsorption amount. The average of the saturation adsorption of oxygen is the largest when the adsorption rate constant, k, is 0.005. The larger the adsorption rate constant, the larger the adsorption amount at adsorption equilibrium. However, the change of the adsorption rate constant has little effect on the time to reach the adsorption equilibrium. That is because the adsorption rate constant is a significant parameter that affects the adsorption efficiency and adsorption ability of the adsorption reaction on the medium surface. A higher adsorption rate constant can make the adsorption intensity of coal higher, and the adsorption occurs evenly. At the same time, more oxygen is adsorbed by the coal, and when the adsorption equilibrium is finally reached, the saturation adsorption amount becomes larger. Figure 10 shows the relationship between adsorption rate constant and the saturation adsorption at different porosites. As can be seen from fig. 10, the saturation adsorptions of different adsorption rate constants are different, showing a monotonically increasing trend. With the increase of porosity, the average value of saturated adsorption amount also shows an upward trend.

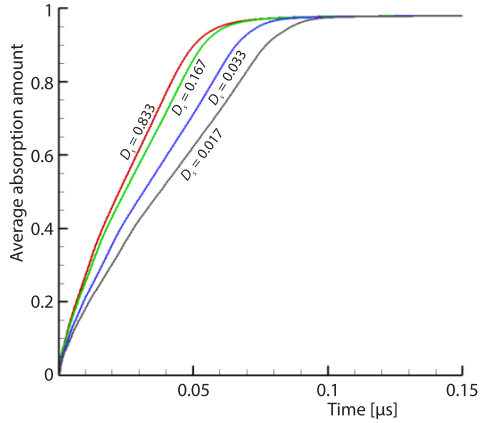

Figure 7. Relationship between different diffusion coefficients and the average adsorption amount

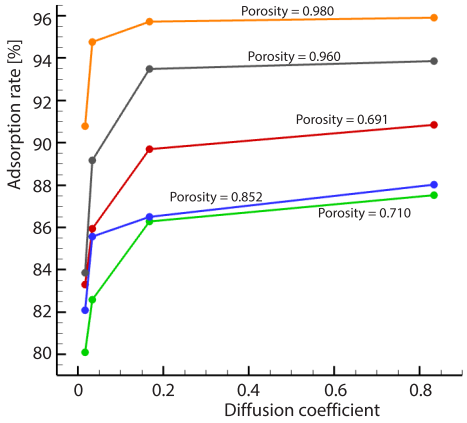

Figure 8. Relationship between diffusion coefficient and adsorption rate under different porosities at 0.055 μs

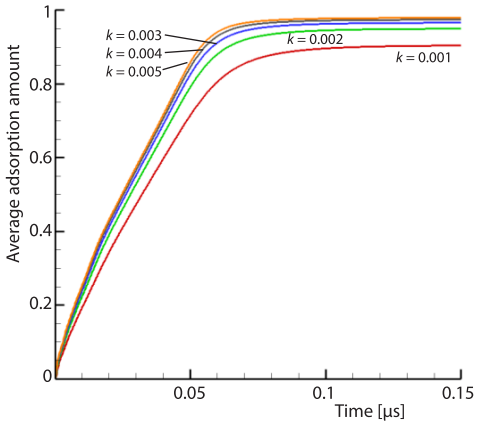

Figure 9. Relationship between adsorption rate constant and the average adsorption amount

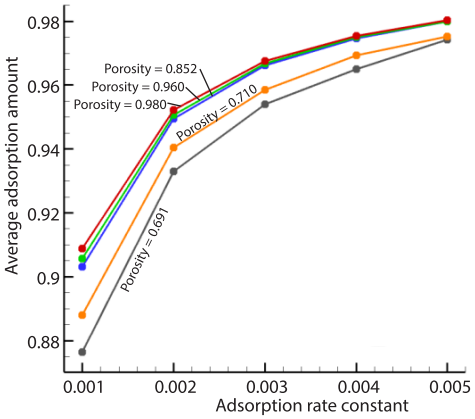

Figure 10. Relationship between adsorption rate constant and the average adsorption amount under different porosities

Pore structure

There has been a long concern about how pore structure affects adsorption behavior in porous media. As show in fig. 11, the adsorption amount of oxygen in equilibrium rises with the fractal dimension. The fractal dimension of coal reflects the intrinsic nature of the surface and pore structure of coal. Because the pore structure of coal with large fractal dimensions is complex, it has a large amount of adsorption. However, when $D_f = 1.746$ and $D_f = 1.893$, the average adsorption amount is obviously larger than that of adjacent fractal dimensions. The $D_f = 1.746$ and its adjacent fractal dimensions $D_f = 1.723$ and $D_f = 1.832$ are divided into group D1, and $D_f = 1.893$ and its adjacent fractal dimensions $D_f = 1.866$ and $D_f = 1.896$ are divided into group D2. Figure 12 is obtained by comparing the relationship between the specific surface area and the average adsorption amount of different fractal dimension models. The figure demonstrates that the relationship between the adsorption amount and the specific surface area is positive linear. This is due to that given the same porosity condition, the coal with a larger specific surface area will form a larger adsorption wall, increasing the contact area between oxygen and coal pores. Pore structure plays a significant role in coal adsorption. Among them, fractal dimension and specific surface area are crucial elements that have an impact on the adsorption behavior.

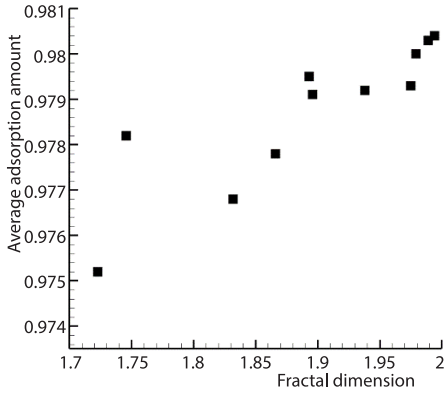

Figure 11. Relationship between fractal dimension and average adsorption amount

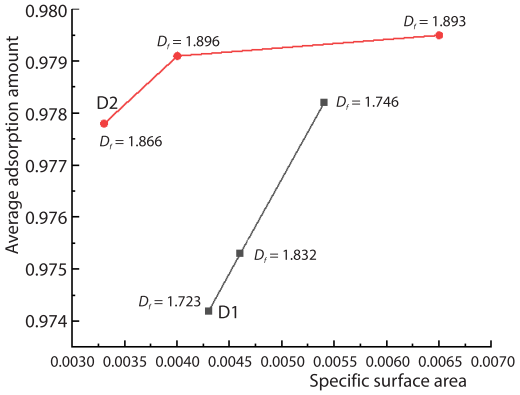

Figure 12. Relationship between specific surface area and average adsorption amount

Conclusions

Combining the fractal dimension of coal with self-similar Sierpinski carpet model, the structural model of coal pores is modeled. Based on the pore-scale, the LBM is used to simulate the process of coal adsorption of oxygen. The effects of oxygen flow dominant channel, diffusion coefficient, adsorption rate constant, and pore structure of coal on the dynamic process of coal oxygen adsorption are analyzed and discussed, and the following conclusions are as follows.

- In the process of oxygen adsorption in coal, oxygen forms a preferential flow in the connecting channel with large pores of coal, and the flow rate of oxygen in the channels far exceeds that of other parts, and the saturated adsorption amount is larger when the adsorption equilibrium is reached.
- The diffusion coefficient controls the spread range of oxygen diffusion, which has a great influence on oxygen concentration distribution. The larger the diffusion coefficient, the higher the adsorption velocity and the shorter the time required for adsorption reach equilibrium.

However, the change of diffusion coefficient has little effect on the saturated adsorption amount when adsorption reaches equilibrium.

- The adsorption rate constant determines the adsorption strength of coal. The larger the adsorption rate constant, the stronger the adsorption ability of coal, and the larger the saturated adsorption amount when the adsorption reaches equilibrium. However, the adsorption rate constant has little effect on the adsorption velocity.
- Pore structure plays a significant role in the adsorption behavior of oxygen in coal. The increase of fractal dimension and specific surface area leads to the increase of saturated adsorption amount when adsorption reaches equilibrium.

Acknowledgment

This work was supported by the Zhejiang Provincial Natural Science Foundation of China [Grant No. LY18E040001].

Nomenclature

C – gas concentration, [molm^{-3}]
C_0 – cutting size, [nm]
c_s – sound speed
D – diffusion coefficient, [m^{2}s^{-1}]
D_f – fractal dimension
$\boldsymbol{e}_i$ – discrete velocity direction
f – distribution function
g – concentration distribution function
k_1 – adsorption rate constant [m^{3}mol^{-1}s^{-1}]
k_{-1} – desorption rate constant, [s^{-1}]
L_0 – side length, [nm]
[M] – matrix
$\boldsymbol{m}$ – velocity moment
N – adsorption amount, [molm^{-3}]
N_m – saturation adsorption amount, [molm^{-3}]
n – order of the Sierpinski carpet model
$\boldsymbol{r}_i$ – particle position
[S] – collision matrix
s_i – relaxation rate
t – time, [μs]
Δt – time step, [μs]
u – velocity in the x-direction, [ms^{-1}]
v – velocity in the y-direction, [ms^{-1}]

Greek symbols

ε – porosity
ν – kinetic viscosity, [m^{2}s^{-1}]
τ – relaxation time
ω – weight coefficient

Superscript

eq – equilibrium
$\hat{}$ – lattice
– – average

Subscripts

i – node
j – node
s – gas
sp – solid

References

[1] Deng, J., *et al.*, Thermophysical Properties of Coal during Low Temperature Oxidation under Different Oxygen Concentrations, *Thermochimica Acta*, *676* (2019), June, pp. 186-197
[2] Wojtacha-Rychter, K., SmoliNski, A., Coal Oxidation with Air Stream of Varying Oxygen Content and fFow Rate-Fire Gas Emission Profile, *Fire Safety Journal*, *116* (2020), 103182
[3] Yuan, L. M., Smith, A. C., The Effect of Ventilation on Spontaneous Heating of Coal, *Journal of Loss Prevention in the Process Industries*, *25* (2012), 1, pp. 131-137
[4] Fang, J. Y., *et al*., Quantitative Analysis of Concrete on the Basis of Fuzzy Set and Computerised Tomography Number, *Thermal Science*, *24* (2020), 6B, pp. 3907-3913
[5] Yu, Z., *et al*., Pore and Fracture Development in Coal under Stress Conditions Based on Nuclear Magnetic Resonance and Fractal Theory, *Fuel*, *309* (2022), 122112
[6] Zou, G. G., *et al.*, Relationship between Micro-Structure and Mechanical Properties of Dissimilar Aluminum Alloy Plates by Friction Stir Welding, *Thermal Science*, *22* (2018), Suppl. 1, pp. S55-S66
[7] Zhou, H. X., *et al*., Evaluating Hydraulic Properties of Biochar-Amended Soil Aggregates by High-Performance Pore-Scale Simulations, *Soil Science Society of America Journal*, *82* (2018), 1, pp. 1-9
[8] Emil, I., *et al*., Microstructure of Titania Aerogels by Reverse Monte Carlo Simulations, *Journal of Physics and Chemistry of Solids*, *168* (2022), 110826

[9] Wei, T., *et al*., Dynamic Brazilian Splitting Experiment of Bedding Shale Based on Continuum-Discrete Coupled Method, *International Journal of Impact Engineering*, *168* (2022), 104289
[10] Hou, P., *et al*., Lattice Boltzmann Simulation of Fluid-Flow Induced by Thermal Effect in Heterogeneity Porous Media, *Thermal Science*, *21* (2017), Suppl. 1, pp. S193-S200
[11] Yu, B. M., Analysis of Flow in Fractal Porous Media, *Applied Mechanics Reviews*, *61* (2008), 5, pp. 050801-050801
[12] Lv, X. Z., *et al*., A Numerical Study on Oxygen Adsorption in Porous Media of Coal Rock Based on Fractal Geometry, *Royal Society Open Science*, *7* (2020), 2, 191337
[13] Ahmadinia, S., *et al*., Forest Chip Drying in Self-Heating Piles during Storage as Affected by Temperature and Relative Humidity Conditions, *Fuel*, *324* (2022), 124419
[14] He, Y. L., *et al*., Lattice Boltzmann Methods for Single-Phase and Solid-Liquid Phase-Change Heat Transfer in Porous Media: A Review, *International Journal of Heat and Mass Transfer*, *129* (2019), Feb., pp. 160-197
[15] Zhou, L., *et al*., Lattice Boltzmann Simulation of the Gas-Solid Adsorption Process in Reconstructed Random Porous Media, *Physical Review E*, *93* (2016), 4, 043101
[16] Wang, H., *et a*l., Coupled GCMC and LBM Simulation Method for Visualizations of CO_2/CH_4 Gas Separation through Cu-BTC Membranes, *Journal of Membrane Science*, *550* (2018), Mar., pp. 448-461
[17] Lei, J, M., *et al.*, Study on Sepage and Adsorption Characteristics of Porous Media Containing Adsorbent Based on Lattice Boltzmann, *AIP Advances*, *11* (2021), 4, 045126
[18] Ning, Y., He, S., Permeability Prediction Considering Surface Diffusion for Gas Shales by Lattice Boltzmann Simulations on Multi-Scale Reconstructed Digital Rocks, *Proceedings*, International Petroleum Technology Conference, Bangkok, Thailand, 2016, Vol. 25, pp. 131-137
[19] Cai, J., Huai, X, L., Study on Fluid-Solid Coupling Heat Transfer in Fractal Porous Medium by Lattice Boltzmann Method, *Applied Thermal Engineering*, *30* (2010), 6-7, pp. 715-723
[20] Pierre, L., Luo, L, S., Theory of the Lattice Boltzmann Method: Dispersion, Dissipation, Isotropy, Galilean Invariance, and Stability, *Physical Review*, *61* (2000), 6, pp. 6546-6562
[21] Guo, Z. L., *et al*., An Extrapolation Method for Boundary Conditions in Lattice Boltzmann Method, *Physical of Fluids*, *14* (2002), 6, pp. 2007-2010

Paper submitted: July 18, 2022
Paper revised: October 1, 2022
Paper accepted: October 26, 2022